

Mapping RNA-Protein Interactions in Ribonuclease P from *Escherichia coli* using Disulfide-linked EDTA-Fe

Roopa Biswas¹, David W. Ledman^{2,3}, Robert O. Fox³, Sidney Altman⁴ and Venkat Gopalan^{1*}

¹Department of Biochemistry
The Ohio State University
Columbus, OH, 43210, USA

²Marketing Department, PE
Biosystems, Inc., Framingham
MA 01701, USA

³Department of Human
Biological Chemistry and
Genetics, The Sealy Center for
Structural Biology, University
of Texas Medical Branch
Galveston, TX, 77555, USA

⁴Department of Molecular
Cellular and Developmental
Biology, Yale University, New
Haven, CT, 06520-8103, USA

The protein subunit of *Escherichia coli* ribonuclease P (which has a cysteine residue at position 113) and its single cysteine-substituted mutant derivatives (S16C/C113S, K54C/C113S and K66C/C113S) have been modified using a sulfhydryl-specific iron complex of EDTA-2-aminoethyl 2-pyridyl disulfide (EPD-Fe). This reaction converts C5 protein, or its single cysteine-substituted mutant derivatives, into chemical nucleases which are capable of cleaving the cognate RNA ligand, M1 RNA, the catalytic RNA subunit of *E. coli* RNase P, in the presence of ascorbate and hydrogen peroxide. Cleavages in M1 RNA are expected to occur at positions proximal to the site of contact between the modified residue (in C5 protein) and the ribose units in M1 RNA. When EPD-Fe was used to modify residue Cys16 in C5 protein, hydroxyl radical-mediated cleavages occurred predominantly in the P3 helix of M1 RNA present in the reconstituted holoenzyme. C5 Cys54-EDTA-Fe produced cleavages on the 5' strand of the P4 pseudoknot of M1 RNA, while the cleavages promoted by C5 Cys66-EDTA-Fe were in the loop connecting helices P18 and P2 (J18/2) and the loop (J2/4) preceding the 3' strand of the P4 pseudoknot. However, hydroxyl radical-mediated cleavages in M1 RNA were not evident with Cys113-EDTA-Fe, perhaps indicative of Cys113 being distal from the RNA-protein interface in the RNase P holoenzyme. Our directed hydroxyl radical-mediated footprinting experiments indicate that conserved residues in the RNA and protein subunit of the RNase-P holoenzyme are adjacent to each other and provide structural information essential for understanding the assembly of RNase P.

© 2000 Academic Press

Keywords: footprinting; RNase P protein subunit; RNA-protein interactions; EPD-Fe; EDTA-Fe

*Corresponding author

Introduction

Ribonuclease P (RNase P) is a member of the ensemble of ribonucleases involved in the maturation of tRNA molecules (Altman & Kirsebom, 1999; Deutscher, 1995; Frank & Pace, 1998). The RNase P holoenzyme in *Escherichia coli* is a ribonucleoprotein (RNP) complex consisting of M1 RNA (377 nucleotides) and C5 protein (119 amino acid residues) (Altman & Kirsebom, 1999; Frank & Pace, 1998). Under certain conditions *in vitro*, M1

RNA (the catalytic subunit) can cleave its substrates even in the absence of its protein cofactor. The processing of precursor tRNA molecules by M1 RNA is significantly enhanced by C5 protein *in vitro* (Altman & Kirsebom, 1999), consistent with the observation that RNase P functions as an RNP complex *in vivo* (Sakano *et al.*, 1974). Recent studies indicate that the protein subunit enhances the affinity of the RNase P holoenzyme for the substrate perhaps by promoting specific interactions with the leader sequence in the substrate (Crary *et al.*, 1998; Kurz *et al.*, 1998; Niranjanakumari *et al.*, 1998; Krummel & Altman, 1999).

Although various biochemical and genetic studies have provided insights into structure-function relationships of both subunits of RNase P from *E. coli* (Altman & Kirsebom, 1999; Frank & Pace, 1998), further progress in elucidating the

Abbreviations used: BABE, 1-(*p*-bromoacetamidobenzyl)-EDTA; CD, circular dichroism; CAP, catabolite activator protein; EPD, EDTA-2-aminoethyl-2-pyridyl disulfide; RNP, ribonucleoprotein.

E-mail address of the corresponding author:
gopalan.5@osu.edu

mechanism of action of RNase P cannot be made without detailed structural data. To date, structural characterization of the RNA subunit in the absence and presence of its pTRNA substrate is based on cumulative information from low resolution techniques such as crosslinking and footprinting (Chen *et al.*, 1998; Christian *et al.*, 1998; Guerrier-Takada *et al.*, 1989; Harris *et al.* 1994, 1998; Kufel & Kirsebom, 1996). Similar studies with the RNase P holoenzyme would be vital for understanding its assembly and mechanism of action. Here, we use an EDTA-Fe-based footprinting approach as a first step in the determination of the spatial orientation of specific parts of the protein cofactor in relation to various domains in the catalytic RNA subunit.

Results

Rationale

The footprinting strategy described in this paper takes advantage of a sulfhydryl-specific EDTA-Fe analog. The iron complex of EDTA-2-aminoethyl 2-pyridyl disulfide (EPD-Fe) is used to attach EDTA-Fe to a single, rationally selected cysteine residue in the protein of interest (Scheme 1; Ermacora *et al.*, 1992, 1994; Hall & Fox, 1999). On reduction of the iron with ascorbate, reactive oxygen species are generated and oxidative degradation of the polypeptide or nucleic acid backbone proximal to the modified residue will occur. Since the reactive species (i.e. the hydroxyl radical) has a very short lifetime in aqueous solution (Ermacora *et al.*, 1996; Tullius, 1987), the radical-mediated chemical cleavages are usually localized and restricted to within 10 Å of the Fe(III) ion. This fact, taken together with the 14 Å tether length of EPD-Fe, implies that information on contact sites derived from this footprinting approach must be viewed as long-range structural probing. EPD-Fe is similar to another metal chelate, the iron complex of 1-(*p*-bromoacetamidobenzyl)-EDTA (BABE-Fe), which has recently been used as a tool to elucidate RNA-protein interactions in HIV-1 Tat-TAR complex (Rana & Meares, 1991; Huq & Rana, 1997) and also to determine the bases in 16 S and 23 S rRNA that are proximal to defined cysteine residues in S4, S5, S13 and L11 ribosomal proteins (Heilek *et al.*, 1995; Heilek & Noller, 1996a,b; Holmberg & Noller,

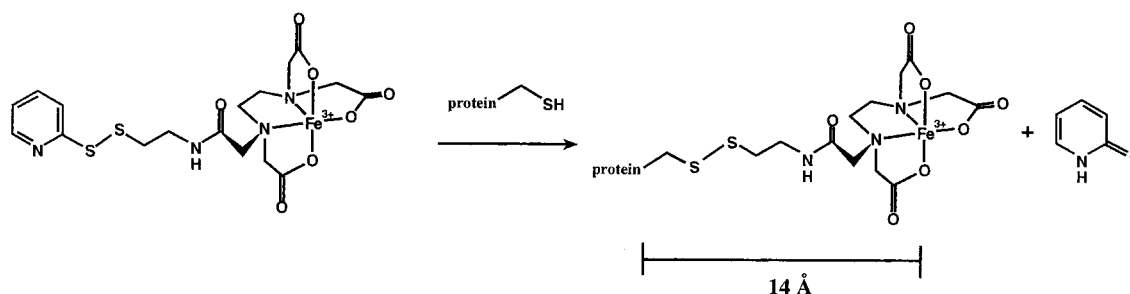
1999). The only difference between BABE-Fe and EPD-Fe is that the latter is more flexible and hydrophilic; therefore, EPD-Fe is expected to produce a more uniform distribution of diffusible free radicals (Hall & Fox, 1999).

EPD-Fe was first designed as a tool to investigate non-native structures of staphylococcal nuclease (Ermacora *et al.*, 1992, 1994, 1996) and subsequently used to map the interactions between the catalytic domain of $\gamma\delta$ resolvase and its DNA substrate (Mazzarelli *et al.*, 1993). In the latter study, the choice of residues for cysteine replacement was based on the crystal structure of the $\gamma\delta$ resolvase (Sanderson *et al.*, 1990; Mazzarelli *et al.*, 1993). The EDTA-Fe-mediated cleavages observed in the $\gamma\delta$ resolvase DNA sites led to a structural model of the $\gamma\delta$ resolvase-DNA complex which was entirely consistent with the structure subsequently established by X-ray crystallography (Yang & Steitz, 1995). No cleavage was observed in the DNA substrates when EDTA-Fe was covalently tethered to a cysteine residue located away from the DNA-protein interface. Similarly, Ebright *et al.* (1992) have independently synthesized and used this reagent for mapping interactions in the catabolite activator protein (CAP)/DNA and Cro/DNA complexes (Ebright *et al.*, 1992). EPD-Fe has also been used to map contact sites between the N-terminal RNA binding domain of human U1A and the 3' UTR of its mRNA (Beck *et al.*, 1998).

Here, we used EPD-Fe to convert C5 protein, or its single cysteine-substituted mutant derivatives, into a chemical nuclease which can in principle cleave its cognate RNA ligand, M1 RNA, and provide a map of contact sites between the two subunits. The success of this strategy depends on: (i) the modification not having an adverse effect on the assembly and function of the RNP complex, and (ii) the modified cysteine residue being at (or near) the RNA-protein interface.

Mutagenesis

Prior to EPD-Fe modification of the single cysteine-substituted mutant derivatives of C5 protein, it is important to rationally select amino acid residues in C5 protein for cysteine mutagenesis. This study was initiated prior to the availability of the tertiary structure of the protein subunit of



Scheme 1.

RNase P. In addition to Cys113 that is present in wild-type C5 protein, the residues Ser16, Lys54 and Lys66 were selected as sites to engineer Cys residues for subsequent modification with EPD-Fe. Ser16 was selected for mutagenesis because of its proximity to the highly conserved residue Phe18. When M1 RNA is reconstituted with the mutant C5 F18A, the resultant mutant holoenzyme displays decreased activity and altered substrate specificity compared to the wild-type holoenzyme (Gopalan *et al.*, 1997). Moreover, C5 F18A displayed weaker binding to M1 RNA compared to the wild-type C5 protein (V.G. & S.A., unpublished results). Since Ser16 was only two residues away from Phe18 and because a Ser to Cys residue substitution causes modest alterations in the chemical character, we chose to replace Ser16 with a Cys residue. Based on the results from our recent EPR spectroscopic studies of M1 RNA-C5 protein interactions, positions 54 and 66 were also selected for Cys mutagenesis modification with EPD-Fe (Gopalan *et al.*, 1999). Although the EPR spectroscopy-based approach facilitated identification of cysteine residues, engineered or otherwise, that might be part of the RNA-protein interface in an RNP complex, it did not yield any information on which residues in M1 RNA are involved in these interactions (Gopalan *et al.*, 1999). The EPD-Fe footprinting experiments reported here were performed to identify nucleotide positions in M1 RNA which are proximal to specific residues (such as 16, 54 and 66) on C5 protein.

Mass spectrometry

The single cysteine residue at position 113 in wild-type C5 protein (Hansen *et al.*, 1985; Figure 1(a)) and in the three single cysteine-substituted mutants (S16C/C113S, K54C/C113S and K66C/C113S) were modified with EPD-Fe (Scheme 1). To examine if the derivatization procedure resulted in covalently tethering Fe-EDTA to C5 protein and its mutant derivatives, electrospray ionization mass spectrometry was used to determine the molecular masses of the various protein samples before and after derivatization with EPD-Fe. The molecular masses observed are in good agreement with the expected values (Table 1). Although we have reported the masses for the protein minus the N-terminal methionine residue, we do observe some species whose masses indicate that the N-terminal methionine residue is present (data not shown). It is likely, therefore, that there is some heterogeneity at the N terminus, as has been observed with other proteins overexpressed in *E. coli* (Dalboge *et al.*, 1990; Sandman *et al.*, 1995).

The extent of derivatization with EPD-Fe was also examined by amino acid analysis. Two of the derivatized protein samples were oxidized with performic acid and hydrolyzed with 6 N HCl for amino acid analysis at the W. M. Keck Foundation Biotechnology Resource Laboratory, Yale University. The oxidation of an EPD-modified cysteine

residue results in formation of cysteic acid and taurine. For a protein sample that is completely derivatized, equimolar amounts of cysteic acid and taurine are expected. Amino acid analysis performed with the protein samples in which residues Cys16 and Cys113 were modified with EPD yielded taurine/cysteic acid ratios of 1.3 and 0.9, respectively. The near-unit ratio of taurine/cysteic acid in our modified protein samples indicate almost complete derivatization.

Circular dichroism spectroscopy

It is conceivable that the cysteine replacements in C5 protein (i.e. S16C, K54C and K66C) and their subsequent modification with EPD-Fe might affect protein folding. CD spectroscopic studies of the unmodified and the EPD-modified mutant derivatives of C5 protein revealed that there were no dramatic alterations in the secondary structure. Although some differences were observed in the CD spectra (Figure 2) between the unmodified and modified C5 protein mutants, the spectra are qualitatively similar. The minor differences between the spectra are likely due to inaccuracies in determining protein concentration, a problem accentuated by a modest, albeit consistent, precipitation of some proteins during the CD measurement. Moreover, deconvolution of the CD spectra of the unmodified and modified proteins yielded similar percentages for the various secondary structural elements (data not shown).

Activity assays

The unmodified and EPD-modified samples of the wild-type C5 protein and its single cysteine-substituted mutants were reconstituted with wild-type M1 RNA and the ability of these holoenzymes to cleave precursor tRNA^{Tyr} (ptRNA^{Tyr}) was examined as described elsewhere (Gopalan *et al.*, 1997). The results of the RNase P assays demonstrated that neither the introduced mutations nor the modification with EPD-Fe significantly alter protein function (Table 2). The wild-type C5 protein when reconstituted with M1 RNA exhibits a catalytic turnover number of 30 min⁻¹. The activities observed with the various mutants are normalized based on the turnover number of the wild-type RNase P holoenzyme. Modification of the C5 protein mutant, K66C/C113S, with EDTA-Fe led to a significant decrease in activity relative to the wild-type protein (Table 2); however, it should be noted that the unmodified mutant protein itself, exhibits a slightly lower activity in comparison to wild-type C5 protein. Nevertheless, this result would imply that some caution is required while interpreting the footprinting results observed with Cys66-EDTA-Fe.

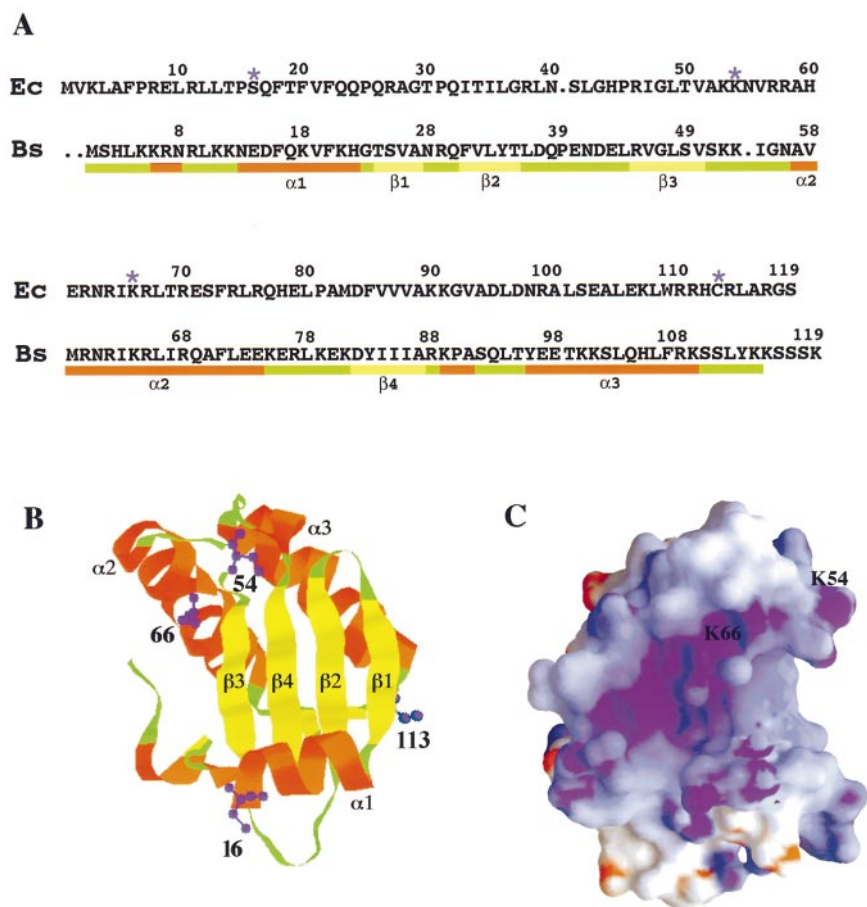


Figure 1. (a) Alignment of the amino acid sequences of the protein subunits of RNase P from *E. coli* and *B. subtilis*. The residues marked by an asterisk indicate sites of cysteine replacement and EPD-Fe modification in the protein subunit of *E. coli* RNase P. The respective secondary structural elements are indicated below the sequence alignment. (b) Tertiary structure of the protein subunit of RNase P from *B. subtilis* (Stams *et al.*, 1998). The program RASMOL was used to depict the α -carbon backbone of the protein structure as a ribbon. The various secondary structural elements are identified using the same color scheme as in (a). The positions where Cys residues were introduced and modified with EPD-Fe are indicated in blue; the numbering is based on the sequence of the protein subunit of *E. coli* RNase P. The program QUANTA'97 *Protein Design* (Molecular Simulations Inc., San Diego) was used to generate the structure of the RNase P protein subunit in which the native amino acid residues at the indicated positions in the *B. subtilis* protein were replaced with a cysteine residue; the coordinates deposited in the PDB by Stams *et al.* (1998) served as the starting template. (c) Electrostatic potential mapped to the molecular surface of the protein depicted in (b); this Figure was prepared using GRASP software (Nicholls, 1993). To reveal the putative RNA-binding central cleft, the view in (c) was obtained by turning the molecule in (b) in a clockwise direction. Blue and red shading represent regions of the surface where basic and acidic residue side-chains would map, respectively. Moreover, K54 and K66 are indicated in (c) to orient the reader while comparing (b) and (c).

Footprinting studies

The footprinting experiments consisted of reconstructing the unmodified and modified protein

samples with either 5' or 3' end-labeled M1 RNA and immediately incubating the holoenzyme complexes individually with ascorbate and hydrogen peroxide. To detect the positions where the

Table 1. Molecular masses of C5 mutants before and after EPD modification as measured by electrospray ionization mass spectrometry

	Before modification		After modification	
	Predicted ^a	Observed	Predicted	Observed
1. Wild-type C5 (C113)	13,658	13,658 (± 1)	14,060	14,061 (± 1)
2. C5 S16C/C113S	13,658	13,659 (± 2)	14,060	14,061 (± 2)
3. C5 K54C/C113S	13,617	13,616 (± 1)	14,019	14,021 (± 2)
4. C5 K66C/C113S	13,617	13,616 (± 2)	14,019	14,021 (± 3)

^a The molecular mass corresponds to that of C5 protein lacking the N-terminal methionine residue.

Table 2. Relative RNase P activity of wild-type C5 protein and its mutant derivatives

C5 Protein	Relative initial velocity (%) ^b
Wild-type C5	100
Wild-type-EDTA-Fe	68(±1)
Cys16 ^a	90(±4)
Cys16-EDTA-Fe	74(±2)
Cys54	89(±2)
Cys54-EDTA-Fe	62(±1)
Cys66	79(±5)
Cys66-EDTA-Fe	28(±3)

^a All cysteine mutants in this Table have an additional change (i.e. C113S).

^b Average of values obtained from two independent experiments.

hydroxyl radical has cleaved the M1 RNA backbone, we used polyacrylamide gel electrophoresis followed by autoradiography. The three EPD-Fe-derivatized proteins, C5 Cys16-EDTA-Fe, Cys54-EDTA-Fe and Cys66-EDTA-Fe, produced specific cleavages in M1 RNA (Figure 3). The failure to

observe a specific hydroxyl radical-mediated cleavage with C5 Cys113-EDTA-Fe implies that residue 113 is distal from the RNA-protein interface in the RNase P holoenzyme (data not shown).

The cleavages in 5' end-labeled M1 RNA observed upon incubation with C5 Cys16-EDTA-Fe, ascorbate and hydrogen peroxide, were restricted to the P3 helix in M1 RNA (Figure 3(a)). After six minutes of incubation of the M1 RNA-C5 Cys16-EDTA-Fe complex with ascorbate and hydrogen peroxide, the first cleavages were observed at positions 49, 50, 51 and 52 in M1 RNA and, albeit weakly, at positions 29, 30 and 31. After a longer incubation (12 minutes), additional cleavages were observed at nucleotide positions 46 through to 48 as well as 53 in M1 RNA (these positions flank the major cleavage sites between 49 and 52). Moreover, there are also cleavages from nucleotide positions 29 through 33. A phosphorimager scan of the dried gel enabled us to quantify the cleavages at individual backbone positions in M1 RNA observed with the underivatized and

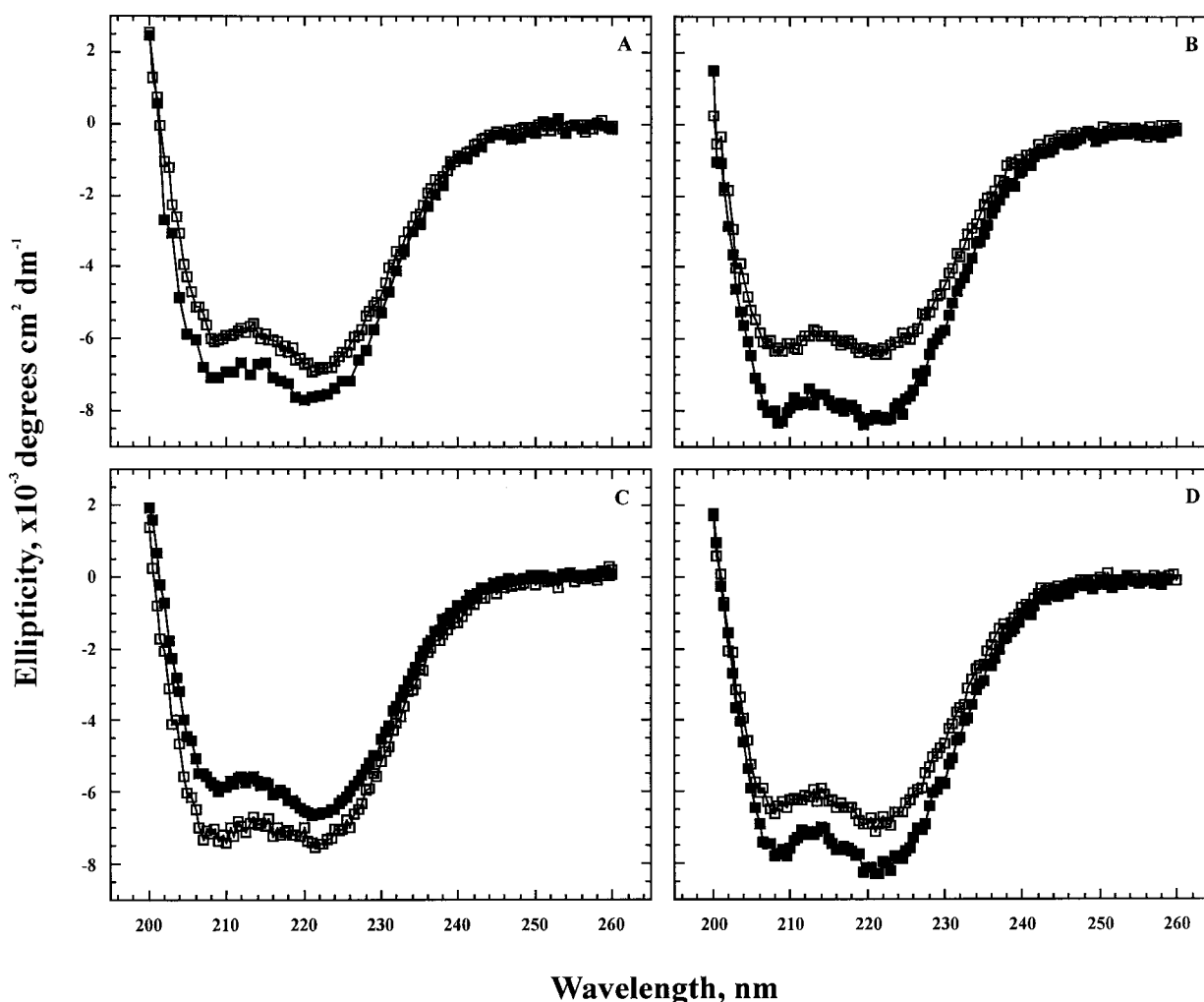


Figure 2. CD spectra of the unmodified (open boxes) and EDTA-Fe-modified (filled boxes) single cysteine-substituted derivatives of C5 protein: (a) wild-type C5 protein, (b) S16C/C113S, (c) K54C/C113S, and (d) K66C/C113S.

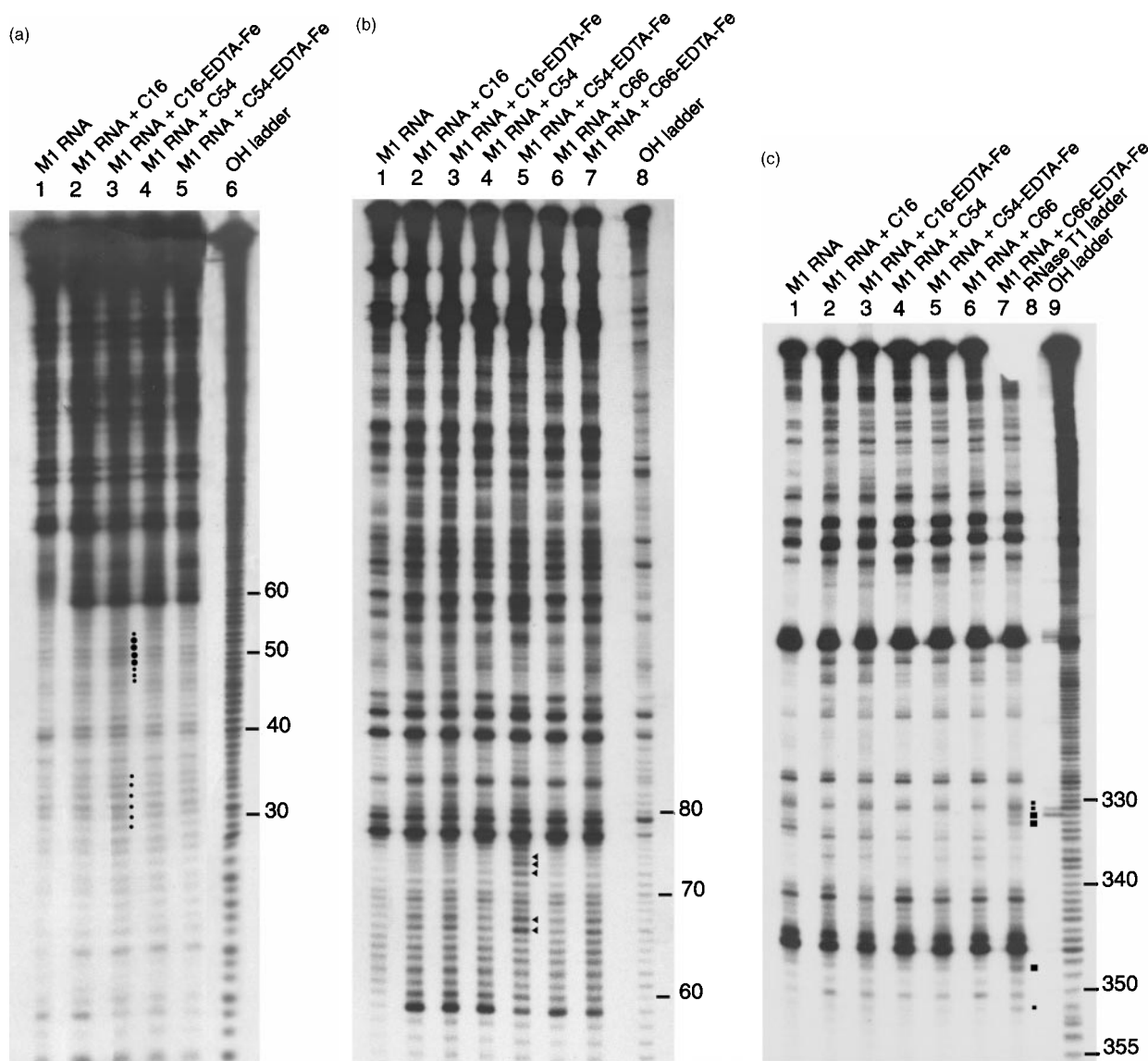


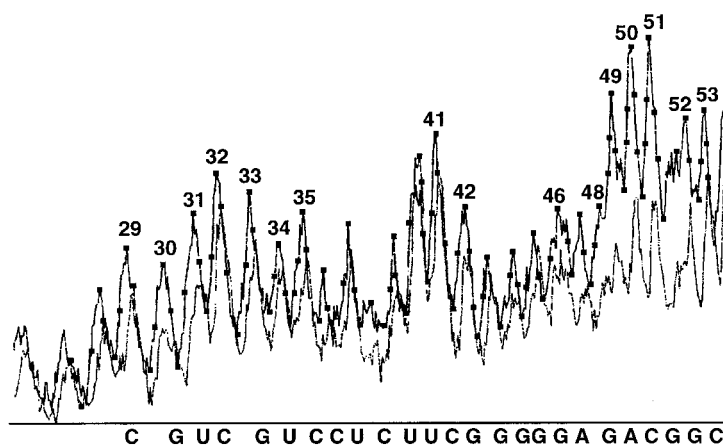
Figure 3. (a) The 5' end-labeled M1 RNA footprints obtained with Cys16-EDTA-Fe. (b) The 5' end-labeled M1 RNA footprints obtained with Cys54-EDTA-Fe. (c) The 3' end-labeled M1 RNA footprints obtained with Cys66-EDTA-Fe. In all three panels, lane 1 represents hydroxyl radical-mediated cleavages on M1 RNA observed in the absence of C5 protein. (a) Lanes 2 and 4 show cleavages on M1 RNA observed with Cys16 and Cys54, respectively, while lanes 3 and 5 show the cleavages promoted by Cys16-EDTA-Fe and Cys54-EDTA-Fe, respectively. In (b) and (c) lanes 2, 4 and 6 show cleavages on M1 RNA when reconstituted with Cys16, Cys54 and Cys66, respectively. Lanes 3, 5 and 7 show the cleavages by Cys16-EDTA-Fe, Cys54-EDTA-Fe and Cys66-EDTA-Fe, respectively, on M1 RNA. The ladders obtained by the alkaline hydrolysis (OH ladder) and RNase T₁ digestion (RNase T₁ ladder) of M1 RNA are indicated.

derivatized protein (Figure 4(a)). It is evident from an inspection of the autoradiogram (compare lane 2 *versus* lane 3 in Figure 3(a)) and the phosphor-imager scan (Figure 4(a)) that when the footprinting reaction is performed with the underivatized protein, the hydroxyl radical-mediated cleavages in M1 RNA are either weak or non-existent. The cleavages at positions 29 through 33 and 46 through 53 are specific to C5 Cys16-EDTA-Fe and were not observed when the footprinting reaction was performed with C5 Cys54-EDTA-Fe or C5 Cys113-EDTA-Fe (lane 5 in Figure 3(a) and data not shown, respectively). The hydroxyl radical-mediated cleavages in M1 RNA observed upon

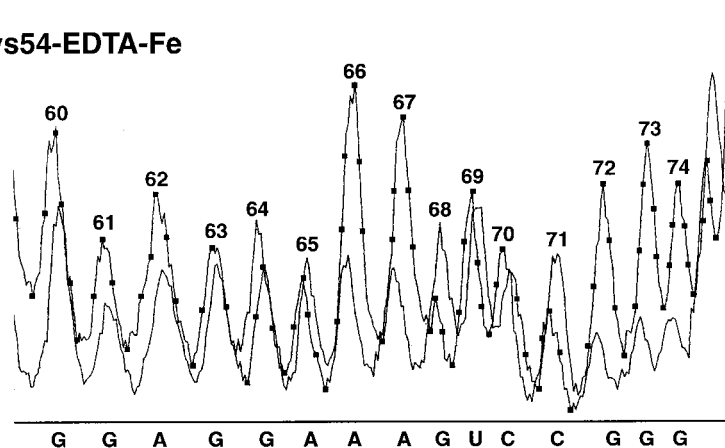
incubation with C5 Cys16-EDTA-Fe were reproducible and consisted of strong and weak cleavages (Figure 3(a)). This pattern would be expected, since the locally generated hydroxyl radicals are diffusible and would be capable of inducing weak secondary cleavages proximal to the primary cleavage sites.

The hydroxyl radical-mediated footprinting observed with Cys54-EDTA-Fe is depicted in Figure 3(b) (lane 5). Prominent cleavages on 5' end-labeled M1 RNA were observed at nucleotides 66, 67 and 72 through 74 after a three-minute incubation with ascorbate and hydrogen peroxide. Weaker cleavages were also observed at nucleotide

A. Cys16-EDTA-Fe



B. Cys54-EDTA-Fe



C. Cys66-EDTA-Fe

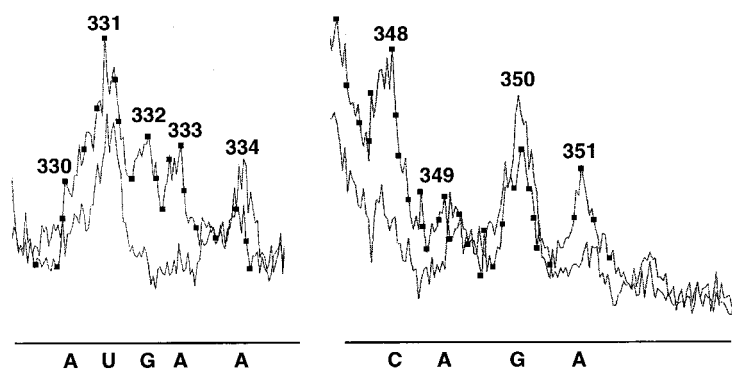


Figure 4. A comparison of the hydroxyl radical-mediated cleavages in M1 RNA promoted by the respective unmodified and EDTA-Fe-modified proteins. Selected regions of the autoradiograms (shown in Figure 3) were scanned with a phosphorimager (Molecular Dynamics) to illustrate the cleavages in M1 RNA promoted by (a) C5 Cys16-EDTA-Fe, (b) C5 Cys54-EDTA-Fe, and (c) C5 Cys66-EDTA-Fe. The numbers indicate the position of the bases in M1 RNA. The corresponding sequence in M1 RNA is also provided. Since the peak heights are in arbitrary units, no scale has been provided for the *y*-axis. The lines with filled symbols refer to scans of the lanes wherein the footprinting reaction was performed with the EDTA-Fe-modified proteins.

positions 60 through 62. The cleavages are restricted to the 5' strand of the P4 pseudoknot. A phosphorimager scan of lanes 4 and 5 in Figure 3(b) is shown in Figure 4(b).

When footprinting experiments were performed using 3' end-labeled M1 RNA and C5 Cys66-EDTA-Fe, prominent cleavages were observed at positions 332 and 333 on M1 RNA after incubation with ascorbate and hydrogen peroxide for three minutes (Figure 3(c), lane 7). Another set of clea-

vages were also observed at nucleotide positions 348 and 351, but these were weaker than those at positions 332 and 333. The weakest cleavages were observed on the flanking nucleotides 330 and 331 as well as 347 and 352. A phosphorimager scan of lanes 6 and 7 in Figure 3(c) is shown in Figure 4(c).

For the various footprinting experiments discussed above, the authenticity of the hydroxyl radical-mediated cleavages was borne out by the consistent increase in intensity of the respective

cleavage products upon prolonged incubation of the reconstituted holoenzymes with ascorbate and hydrogen peroxide (data not shown).

In contrast to the specific and distinct cleavages obtained with 3' end-labeled M1 RNA, incubation of 5' end-labeled M1 RNA with Cys66-EDTA-Fe led to weak, random cleavages at several positions proximal to the 5' end of M1 RNA (data not shown). Although there appears to be no major secondary structural alterations in the modified protein (Cys66-EDTA-Fe) compared to its unmodified counterpart (Figure 2(d)), it is possible that the mutation and modification of a highly conserved residue (i.e. K66C) compromises RNase P holoenzyme assembly and this underlies the non-specific cleavage pattern observed with C5 Cys-66-EDTA-Fe and 5' end-labeled M1 RNA.

Discussion

A footprinting strategy involving site-specific modification of C5 protein into a chemical nuclease has been used to map its contact sites with M1 RNA, the catalytic RNA subunit of *E. coli* RNase P.

Selected residues on C5 protein were mutated to cysteine and reacted with the thiol-specific chemical reagent EPD-Fe. The modification of single cysteine-substituted mutant derivatives of C5 protein with EPD-Fe was confirmed by mass spectrometry (Table 1). To ensure that the mutation of selected residues to Cys residues and the subsequent modification of these Cys residues with EPD-Fe did not interfere with the structure and function of the protein, CD spectroscopic analyses and RNase P activity assays were performed. The observation that the CD spectra of the unmodified and the respective EDTA-Fe-modified mutant derivatives of C5 protein are similar confirmed that the EDTA-Fe modification did not alter the structure significantly (Figure 2). The RNase P activity assays revealed a noticeable decrease in activity in only one case; upon covalently tethering EDTA-Fe to Cys66, the RNase P activity was one-quarter that observed with the wild-type C5 protein (Table 2). This result highlights a limitation of our footprinting strategy. To obtain information on contact sites in an RNP complex, it is necessary to introduce EDTA-Fe proximal to the RNA-protein interface; however, the introduction of EDTA-Fe proximal to residues (in the protein cofactor) that are important for RNA-protein interactions in RNase P might annul interactions essential for RNase P activity. Since there was significant activity even after modification of Cys66, we have proceeded with footprinting experiments using C5 Cys66-EDTA-Fe (see below). However, it would be desirable if the results obtained with C5 Cys66-EDTA-Fe are independently confirmed with another single cysteine-substituted mutant derivative in which the Cys residue is introduced at a position proximal to Lys66.

The EPD-modified single cysteine-substituted mutants of C5 protein were reconstituted with M1 RNA. The hydroxyl radicals generated upon incubation of ascorbate and hydrogen peroxide with the EDTA-Fe-modified RNase P holoenzymes were expected to cleave the M1 RNA backbone proximal to the site of modification in C5 protein. The M1 RNA cleavage patterns observed with Cys16-, Cys54-, and Cys66-EDTA-Fe are summarized in Figure 5. As cautioned by Hall & Fox (1999), these hydroxyl radical-mediated cleavage sites in the RNA do not correspond to sites of direct interaction with the protein subunit. Since the EDTA-Fe moiety and the ribose units in the RNA must be within 10 Å and appropriately oriented for cleavage, it is reasonable to conclude that the cleavages we observed in M1 RNA map nucleotides which are proximal to residues 16, 54 and 66 in C5 protein (when the two subunits are assembled into the RNase P holoenzyme). Cys113-EDTA-Fe failed to promote hydroxyl radical-mediated cleavages in M1 RNA, indicating that this residue is not at the RNA-protein interface in the RNase P holoenzyme complex (data not shown). Consistent with this observation, the tertiary structure of C5 protein places Cys113 (in α 3-helix) behind the putative RNA-binding central cleft and predicts it to be distal from the RNA-protein interface (Figure 1(b); see discussion below).

Our studies indicate that C5 Cys16-EDTA-Fe cleaved nucleotides 49, 50, 51 and 52 in the P3 helix of M1 RNA (Figure 5(a)). Phylogenetic sequence analysis has led to inclusion of the P3 helix in the minimal consensus structure of the RNase P RNA subunit. However, there are no conserved nucleotides in the P3 helix. It is possible that the hydroxyl radical-mediated cleavages in the P3 region that we observed with Cys16-EDTA-Fe might merely reflect the physical juxtaposition of α 1-helix in C5 protein and the P3 paired region in M1 RNA, rather than specific RNA-protein interactions between these regions. A separate photochemical crosslinking experiment has also yielded results suggesting that the P3 helix of M1 RNA might be adjacent to the protein in the RNase P holoenzyme. M1 RNA with randomly incorporated photoactivatable nucleotides was crosslinked to C5 protein to determine the sites of contact between M1 RNA and C5 protein (C. Guerrier-Takada & S.A., unpublished results). When the crosslinked complex was isolated and subjected to a primer extension analysis with reverse transcriptase, the crosslinks between M1 RNA and C5 protein involved bases in the P3 helix of M1 RNA. Moreover, the observation that a 4-thiouridine residue at position -10 in the 5' leader of the pRNA substrate crosslinks to C50 in the P3 helix suggests the physical vicinity of P3 in M1 RNA and the substrate during RNase P catalysis (Christian & Harris, 1999).

When Cys54-EDTA-Fe was used in the footprinting experiments, the hydroxyl radical-mediated cleavages were localized to nucleotides 66, 67 and

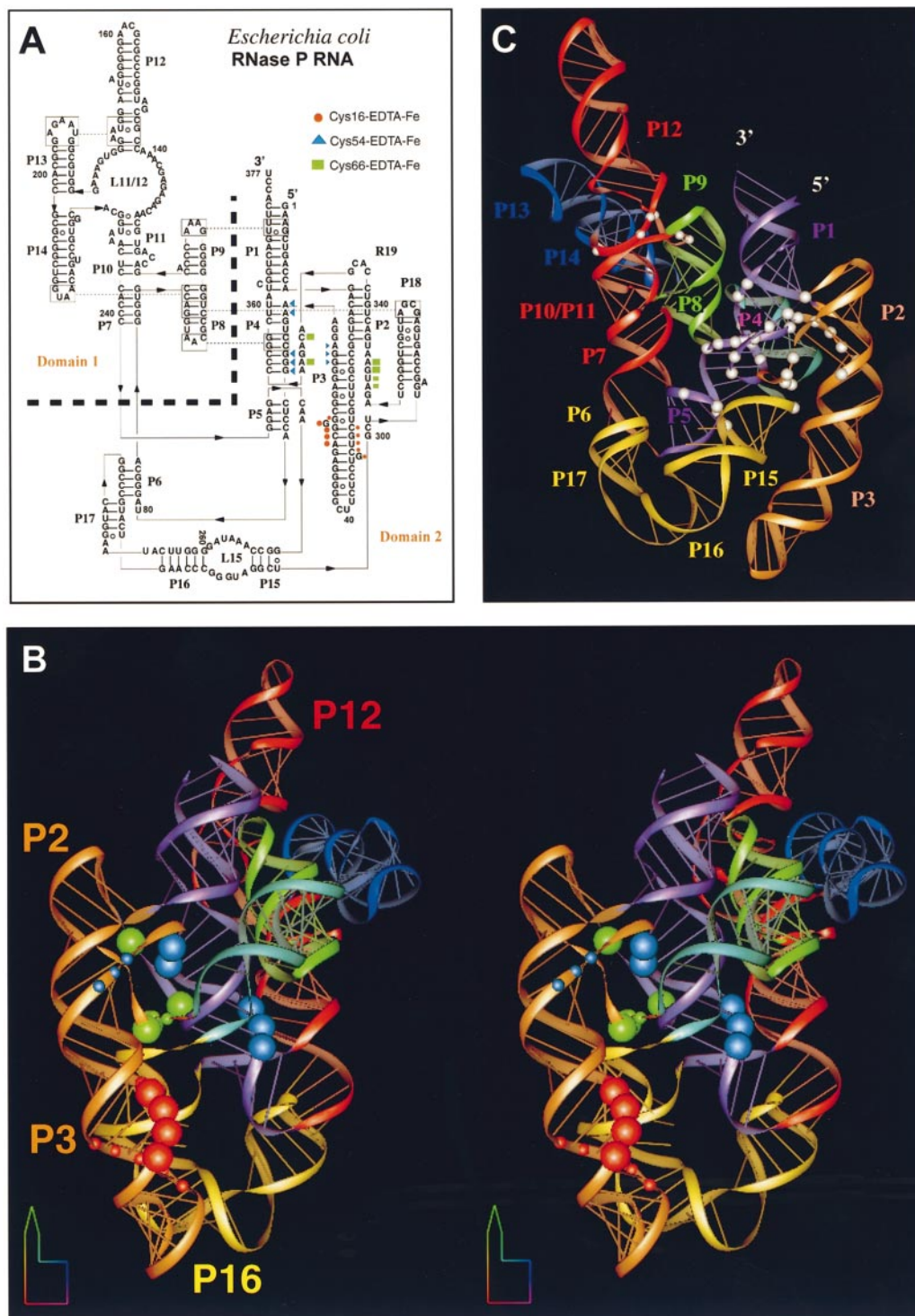


Figure 5. (a) The hydroxyl radical-mediated cleavages in M1 RNA promoted by C5 Cys16-, Cys54- and Cys66-EDTA-Fe are denoted by circles (red), triangles (blue) and squares (green), respectively. The size of the symbols corresponds to the intensity of the hydroxyl radical-mediated cleavages. The secondary structure representation and the numbering of helices of M1 RNA are as described by Massire *et al.* (1998). (b) A stereoview representation depicting the hydroxyl radical-mediated cleavages in the tertiary structure model of M1 RNA (Massire *et al.*, 1998). The cleavage sites are shown as spheres using the same color code as in (a). (c) Large white spheres indicate the invariant nucleotides in the putative active site of M1 RNA (Massire *et al.*, 1998). The view in (c) was obtained by rotating 180° clockwise the molecule in (b). Figures in (b) and (c) were generated using the software DRAWNA (Massire *et al.*, 1994).

72 to 74 of the 5' strand of the P4 pseudoknot (Figure 5(a)). When the EDTA-Fe probe was attached to Cys66, prominent cleavages were observed at positions 332 and 333 (in J18/2) as well as 348 and 351 (in J2/4) (Figure 5(a)). Intramolecular crosslinking studies have confirmed that the J18/2 region is close to J2/4 (Harris *et al.*, 1994). Since residues Lys54 and Lys66 are proximal in the tertiary structure of C5 protein, it is not surprising to find that directed hydroxyl radical-mediated cleavages by Cys54- and Cys66-EDTA-Fe are at adjacent positions in the proposed three-dimensional structure of M1 RNA (Figure 5(b)). This structure represents a computer-aided model based in part on conclusions from phylogenetic covariation analysis and crosslinking data (Massire *et al.*, 1998).

It is instructive to interpret the footprinting results with Cys54- and Cys66-EDTA-Fe based on: (i) results from chemical-modification interference, as well as crosslinking studies that have sought to establish the active site in M1 RNA; and (ii) the three-dimensional structure of the protein subunit of *Bacillus subtilis* RNase P.

Using Rp-phosphorothioates in modification-interference experiments, Harris & Pace (1995) determined that replacement of a non-bridging oxygen atom with a sulfur atom at the phosphates 5' of M1 RNA nucleotides A67, G68, U69 and A352 (in the P4 pseudoknot) led to a dramatic reduction in catalytic activity and that these phosphate groups were therefore likely to represent metal-binding sites important for RNase P catalysis. A similar approach was used by Hardt *et al.* (1995) while deriving their conclusion that phosphates 5' of M1 RNA nucleotides A67, G68, U69, C70, C71 (in the 5'-strand of P4), A130, A132, A248, A249, G300, A317, A330 (in J18/2), A352 (in J2/4), C353 and C354 (in the 3' strand of P4) were important for tRNA binding. Dimethylsulfate-based chemical footprinting experiments have revealed that G332 in M1 RNA is protected from chemical modification by a precursor tRNA substrate which contains a four-nucleotide sequence (LaGrandeur *et al.*, 1994). This observation was further supported by the observation that a long-range photoagent (azidophenacyl bromide) at position 332 of M1 RNA led to intermolecular crosslinking with nucleotides -4 and -5 in the leader sequence of ptRNA (Harris *et al.*, 1994). In a complementary approach, short-range crosslinking experiments using 4-thiouridine at -1 in the leader sequence demonstrated convincingly that G332 and A333 on M1 RNA must be in close contact with the nucleotide at the -1 position of the ptRNA substrate (Kufel & Kirsebom, 1996). Although these studies used the catalytic RNA subunit (i.e. M1 RNA) and not the RNase P holoenzyme complex (i.e. M1 RNA and C5 protein), it is evident that the J18/2 region, which includes nucleotides 332 and 333, interacts with the 5' leader in the ES complex.

The results from various experimental approaches mentioned above attest to the pivotal

role of the regions P4, J18/2 and J2/4 (in M1 RNA) in RNase P catalysis and lend significance to the directed hydroxyl radical-mediated footprints in P4, J18/2 and J2/4 that were observed with C5 Cys54- and Cys66-EDTA-Fe.

Recently, the tertiary structure of the RNase P protein subunit from *B. subtilis* has been determined (Stams *et al.*, 1998). The overall topology is $\alpha\beta\beta\alpha\beta\alpha$ and it includes the presence of an uncommon $\beta\alpha\beta$ left-handed crossover connection from $\beta 3$ to $\alpha 2$ to $\beta 4$ (Figure 1(b)). The structure of the protein subunit of RNase P reveals that most of the conserved residues are present in two regions: (i) the large central cleft (20 Å long and 10 Å wide) which is formed by packing of the helix $\alpha 1$ against the β -sheet; and (ii) helix $\alpha 2$ as well as the loop which precedes it in the $\beta\alpha\beta$ left-handed crossover motif (Figure 1(b)). The surface electrostatic potential map of this protein reveals a cleft rich in positively charged residues (Figure 1(c)). Therefore, this large cleft could play a role in binding either the catalytic RNA subunit or the ptRNA substrate or both. Since there is a high degree of sequence homology between the protein subunits of RNase P from *E. coli* and *B. subtilis*, it is likely that the two proteins will adopt a similar tertiary structure. Therefore, the highly conserved residues Lys54 and Lys66 will likely line the basic cleft in the tertiary structure of the protein subunit of *E. coli* RNase P. Since the hydroxyl radical-mediated cleavages promoted by Cys54- and Cys66-EDTA-Fe occur adjacent to or in conserved nucleotides (such as A66, G332 and A351) that are part of the putative active site of M1 RNA, RNA-protein interactions in RNase P likely involve conserved residues in both M1 RNA and C5 protein.

Results from kinetic studies have led Fierke and co-workers to conclude that the protein component of RNase P functions mainly to facilitate substrate binding by the RNase P holoenzyme (Kurz *et al.*, 1998). A recent crosslinking study using the RNase P holoenzyme from *B. subtilis* demonstrated that the residues in the central cleft of the protein cofactor are proximal to the ptRNA leader sequence under certain conditions *in vitro* (Niranjanakumari *et al.*, 1998). Our observations show that Lys54 and Lys66 (which line the central cleft) are proximal to P4 and J18/2 in M1 RNA, respectively, suggesting that the binding cleft in C5 protein is adjacent to the active site in M1 RNA and presumably to the cleavage site in the ptRNA substrate during RNase P catalysis. Specific interactions between the RNA subunit and the protein cofactor might constrain conserved nucleotides in M1 RNA, perhaps essential for metal binding, and thus position them for optimal interactions with the ptRNA substrate.

Our directed hydroxyl radical-mediated footprinting experiments using the RNase P holoenzyme have identified nucleotides in M1 RNA that are proximal to specific sites in C5 protein and provide a framework for understanding the assembly of the RNase P holoenzyme. Extending this footprinting approach to the ternary complex formed

by the RNase P holoenzyme and the ptRNA substrate will provide structural information on the holoenzyme-substrate complex.

Materials and Methods

Mutagenesis, purification and EPD-Fe modification of mutant derivatives of C5 protein

Details of site-directed mutagenesis of C5 protein, overexpression and purification of mutant derivatives in BL21 (DE3) or T7 A49 *E. coli* cells are provided elsewhere (Gopalan *et al.*, 1997, 1999). After purification of the various mutant derivatives of C5 protein, we verified that the sulfhydryl groups in the various protein samples were accessible to modification with the Ellman reagent (Means & Feeney, 1971). Subsequently, the modification reactions were performed in 50 mM sodium acetate, 10 mM magnesium acetate, 7 M urea (pH 7.2), to ensure complete derivatization of the cysteine residues. The reaction was carried out at 25 °C for 60 minutes using a twofold excess of EPD-Fe over the protein concentration. The samples were dialyzed (after modification) to remove any unreacted EPD-Fe.

Mass spectrometry

Mass spectra were acquired using a Fisons VG platform single quadrupole mass spectrometer with an electrospray ionization source. Instrument configuration, voltage settings, resolution settings, and data processing parameters were as described (Ledman & Fox, 1997; Platis *et al.*, 1993). The sample preparation, calibration method and acquisition parameters are provided elsewhere (Bhat *et al.*, 1997). The only difference between the latter report and this study was that the protein samples contained 250 mM acetic acid and protein concentrations ranged from 1 to 8 pmol/ml. For HPLC-ESI-MS, the source temperature was increased to 150 °C and the continuum data acquisition mode was used. A total of 1 mg of protein was injected into the HPLC system and run over a Vydac 218Tp52 C18 reversed-phase column at 0.2 ml/minute and eluted in a linear gradient from 20 % to 60 % solvent B. Solvents A and B were 0.1 % formic acid with 10 mM ammonium acetate and 0.1 % formic acid with acetonitrile, respectively.

Circular dichroism spectroscopy

The unmodified protein samples were treated with tenfold excess DTT at 4 °C for one hour. Both the EDTA-Fe-modified and unmodified samples (500 μ l) at concentrations of 24 μ M were dialyzed against 10 mM potassium phosphate buffer (pH 7.0) and 400 mM potassium chloride. The freshly dialyzed samples were immediately used for CD spectroscopic analysis. A cuvette of 1 mm path length was used. The measurements were performed using an Aviv Instruments CD spectrophotometer. The wavelength scans were performed from 200 to 260 nm, with a scan speed of 0.5 nm every second. For each sample, the average values obtained from five scans were used to derive the final spectra. Subsequent to blank corrections, the raw ellipticity values were converted to molar ellipticity values by using the appropriate protein concentrations.

Footprinting experiments

The first step in our experiments involves renaturation of M1 RNA. The *in vitro* transcribed, end-labeled sample of M1 RNA was subjected to a five minute denaturation procedure at 65 °C in 10 mM Hepes, 10 mM magnesium acetate, 400 mM ammonium acetate, 0.01 % (v/v) NP-40 (pH 7.5), and then allowed to renature by cooling the sample to room temperature. The footprinting reaction mixtures (50 μ l) consisted of 4 nM 5' or 3' end-labeled (50,000 cpm), renatured M1 RNA and 40 nM of unmodified or modified C5 protein. After a ten minute preincubation at 37 °C to promote RNase P holoenzyme complex formation, the complex was kept on ice for ten minutes. Meanwhile, stocks of ascorbate (ALDRICH) and thiourea (SIGMA) were freshly prepared. A fresh stock of hydrogen peroxide (3%; MALLINCKRODT) was used for these footprinting experiments. The cleavage reactions were initiated by addition of 5.5 μ l of a mixture of 25 mM ascorbate and 1 % (v/v) hydrogen peroxide yielding final concentrations of 2.5 mM and 0.1 %, respectively. The cleavage reactions were carried out on ice. After six minutes, an aliquot of 27 μ l was withdrawn and added to a 1.5 ml tube containing 3 μ l of 0.2 M thiourea, vortexed and quickly immersed in a dry ice/acetone bath. This procedure was followed to obtain the samples after 12 minutes of incubation on ice. The RNA samples were then precipitated using sodium acetate and ethanol and washed twice with 70 % (v/w) ethanol. The dried RNA was resuspended in urea dye and loaded on an 8 % or 10 % denaturing polyacrylamide gel. The gels were dried, scanned using a phosphorimager (Molecular Dynamics, model 445 SI) and quantified using the software ImageQuaNT (version 4.1).

Acknowledgments

We are grateful to Dr Cecilia Guerrier-Takada for generously supplying reagents, for helpful discussions and for kindly consenting to our citing her unpublished results. We thank Professor Eric Westhof, CNRS, Strasbourg, for his generous assistance in preparation of Figure 5. We appreciate the help of Dr Ramesh Kekuda with protein purification and Tim Eubank with graphics. Research in the laboratory of S.A. is supported by National Institutes of Health grant GM19422 and a Human Frontier Science Program grant RG 0291. Research in the laboratory of R.O.F. is supported by National Institutes of Health grants GM51332 and GM55851, the Welch Foundation and the Department of Human Biological Chemistry and Genetics Structural Biology Program, University of Texas Medical Branch. Research in the laboratory of V.G. is supported by grants from the Ohio-W. Virginia Affiliate of the American Heart Association and by a Seed Grant from the OSURF. R.B. is supported by a postdoctoral fellowship from the Ohio-W. Virginia Affiliate of the American Heart Association.

References

- Altman, S. & Kirsebom, L. (1999). Ribonuclease P. In *The RNA World* (Gesteland, R. F., Cech, T. & Atkins, J. F., eds), pp. 351-380, Cold Spring Harbor Laboratory Press, Cold Spring Harbor, NY.

- Beck, D. L., Stump, W. T. & Hall, K. B. (1998). Defining the orientation of the human U1A RBD1 on its UTR by tethered-EDTA(Fe) cleavage. *RNA*, **4**, 331-339.
- Bhat, M. G., Ganley, L. M., Ledman, D. W., Goodman, M. A. & Fox, R. O. (1997). Stability studies of amino acid substitutions at tyrosine 27 of the staphylococcal nuclease β -barrel. *Biochemistry*, **36**, 12167-12174.
- Chen, J. L., Nolan, J. M., Harris, M. E. & Pace, N. R. (1998). Comparative photocross-linking analysis of the tertiary structures of *Escherichia coli* and *Bacillus subtilis* RNase P RNAs. *EMBO J.* **17**, 1515-1525.
- Christian, E. L. & Harris, M. E. (1999). The track of the pre-tRNA 5' leader in the ribonuclease P ribozyme-substrate complex. *Biochemistry*, **38**, 12629-12638.
- Christian, E. L., McPheeters, D. S. & Harris, M. E. (1998). Identification of individual nucleotides in the bacterial ribonuclease P ribozyme adjacent to the pre-tRNA cleavage site by short-range cross-linking. *Biochemistry*, **37**, 17618-17628.
- Crary, S. M., Niranjanakumari, S. & Fierke, C. A. (1998). The protein component of *Bacillus subtilis* RNase P increases catalytic efficiency by enhancing interactions with the 5' leader sequence of pre-tRNA^{Asp}. *Biochemistry*, **37**, 9409-9416.
- Dalboge, H., Byane, S. & Pedersen, J. (1990). *In vivo* processing of N-terminal methionine in *Escherichia coli*. *FEBS Letters*, **266**, 1-3.
- Deutscher, M. P. (1995). tRNA processing nucleases. In *tRNA: Structure, Biosynthesis and Function* (Söll, D. & Raj Bhandary, U., eds), pp. 51-65, American Society for Microbiology, Washington, DC.
- Ebright, Y. W., Chen, Y., Pendergrast, P. S. & Ebright, R. H. (1992). Incorporation of an EDTA-metal complex at a rationally selected site within a protein: application to EDTA-iron DNA affinity cleaving with catabolite activator protein (CAP) and Cro. *Biochemistry*, **31**, 10664-10670.
- Ermacora, M. R., Delfino, J. M., Cuenoud, B., Schepartz, A. & Fox, R. O. (1992). Conformation-dependent cleavage of staphylococcal nuclease with a disulfide-linked iron chelate. *Proc. Natl Acad. Sci. USA*, **89**, 6383-6387.
- Ermacora, M. R., Ledman, D. W., Hellinga, H. W., Hsu, G. W. & Fox, R. O. (1994). Mapping staphylococcal nuclease conformation using an EDTA-Fe derivative attached to genetically engineered cysteine residues. *Biochemistry*, **33**, 13625-13641.
- Ermacora, M. R., Ledman, D. W. & Fox, R. O. (1996). Mapping the structure of a non-native state of staphylococcal nuclease. *Nature Struct. Biol.* **3**, 59-66.
- Frank, D. N. & Pace, N. R. (1998). Ribonuclease P: unity and diversity in a tRNA processing ribozyme. *Annu. Rev. Biochem.* **67**, 153-180.
- Gopalan, V., Baxeavanis, A., Landsman, D. & Altman, S. (1997). Functional analysis of conserved amino acid residues in the protein subunit of ribonuclease P from *Escherichia coli*. *J. Mol. Biol.* **267**, 818-829.
- Gopalan, V., Kühne, H., Biswas, R., Li, H., Brudvig, G. W. & Altman, S. (1999). Mapping RNA-protein interactions in ribonuclease P from *Escherichia coli* using electron paramagnetic resonance spectroscopy. *Biochemistry*, **38**, 1705-1714.
- Guerrier-Takada, C. & Altman, S. (1992). Reconstitution of enzymatic activity from fragments of M1 RNA. *Proc. Natl Acad. Sci. USA*, **89**, 6383-6387.
- Guerrier-Takada, C., Lumelsky, N. & Altman, S. (1989). Specific interactions in RNA enzyme-substrate complexes. *Science*, **286**, 1578-1584.
- Haas, E. S., Brown, J. W., Pitulle, C. & Pace, N. R. (1994). Further perspective on the catalytic core and secondary structure of ribonuclease P RNA. *Proc. Natl Acad. Sci. USA*, **91**, 2527-2531.
- Hall, K. B. & Fox, R. O. (1999). Directed cleavage of RNA with protein-tethered EDTA-Fe. *Methods: Comp. Methods Enzymol.* **18**, 78-84.
- Hansen, F. G., Hansen, E. G. & Atlung, T. (1985). Physical mapping and nucleotide sequence of the *rnpA* gene that encodes the protein component of ribonuclease P in *Escherichia coli*. *Gene*, **38**, 85-93.
- Hardt, W.-D., Warnecke, J. M., Erdmann, V. A. & Hartmann, R. K. (1995). Rp-phosphorothioate modifications in RNase P RNA that interfere with tRNA binding. *EMBO J.* **14**, 2935-2944.
- Harris, M. E. & Pace, N. R. (1995). Identification of phosphates involved in catalysis by the ribozyme RNase P RNA. *RNA*, **1**, 210-218.
- Harris, M. E., Nolan, J. M., Malhotra, A., Brown, J. W., Harvey, S. C. & Pace, N. R. (1994). Use of photoaffinity crosslinking and molecular modeling to analyze the global architecture of ribonuclease P RNA. *EMBO J.* **13**, 3953-3963.
- Harris, M. E., Frank, D. N. & Pace, N. R. (1998). Structure and catalytic function of the bacterial ribonuclease P ribozyme. In *RNA Structure and Function* (Simons, R. W. & Grunberg-Manago, M., eds), Cold Spring Harbor Laboratory Press, Cold Spring Harbor, NY.
- Heilek, G. & Noller, H. F. (1996a). Site-directed hydroxyl radical probing of the rRNA neighborhood of ribosomal protein S5. *Science*, **272**, 1659-1662.
- Heilek, G. & Noller, H. F. (1996b). Directed hydroxyl radical probing of the rRNA neighborhood of ribosomal protein S13 using tethered Fe(II). *RNA*, **2**, 597-602.
- Heilek, G., Marousak, R., Meares, C. F. & Noller, H. F. (1995). Directed hydroxyl radical probing of 16S rRNA using Fe(II) tethered to ribosomal protein S4. *Proc. Natl Acad. Sci. USA*, **92**, 1113-1116.
- Holmberg, L. & Noller, H. F. (1999). Mapping the ribosomal RNA neighborhood of protein L11 by directed hydroxyl radical probing. *J. Mol. Biol.* **289**, 223-233.
- Huq, I. & Rana, T. M. (1997). Probing the proximity of the core domain of HIV-1 Tat fragment in a Tat-TAR complex by affinity cleaving. *Biochemistry*, **36**, 12592-12599.
- Krummel, D. A. P. & Altman, S. (1999). Multiple binding modes of substrate to the catalytic RNA subunit of RNase P from *Escherichia coli*. *RNA*, **5**, 1021-1033.
- Kufel, J. & Kirsebom, L. A. (1996). Different cleavage sites are aligned differently in the active site of M1 RNA, the catalytic subunit of *Escherichia coli* RNase P. *Proc. Natl Acad. Sci. USA*, **93**, 6085-6090.
- Kurz, J. C., Niranjanakumari, S. & Fierke, C. A. (1998). Protein component of *Bacillus subtilis* RNase P specifically enhances the affinity for precursor-tRNA^{Asp}. *Biochemistry*, **37**, 2393-2400.
- LaGrandeur, T. E., Huttenhofer, A., Noller, H. F. & Pace, N. R. (1994). Phylogenetic comparative chemical footprint analysis of the interaction between ribonuclease P RNA and tRNA. *EMBO J.* **13**, 3945-3952.
- Ledman, D. W. & Fox, R. O. (1997). Water cluster calibration reduces mass error in electrospray ionization mass spectrometry of proteins. *J. Am. Soc. Mass. Spectrom.* **8**, 1158-1164.

- Massire, C., Gaspin, C. & Westhof, E. (1994). DRAWNA: a program for drawing schematic views of nucleic acids. *J. Mol. Graph.* **12**, 201-206.
- Massire, C., Jaeger, L. & Westhof, E. (1998). Derivation of the three-dimensional architecture of bacterial ribonuclease P RNAs from comparative sequence analysis. *J. Mol. Biol.* **279**, 773-793.
- Mazzarelli, J. M., Ermacora, M. R., Fox, R. O. & Grindley, N. D. F. (1993). Mapping interactions between the catalytic domain of resolvase and its DNA substrate using cysteine-coupled EDTA-iron. *Biochemistry*, **32**, 2979-2986.
- Means, G. E. & Feeney, R. E. (1971). In *Chemical Modification of Proteins*, pp. 155-157, Holden-Day, San Francisco.
- Nicholls, A. (1993). *GRASP: Graphical Representation and Alignment of Surface Properties*, Columbia University, New York.
- Niranjanakumari, S., Stams, T., Crary, S. M., Christianson, D. W. & Fierke, C. (1998). Protein component of the ribozyme ribonuclease P alters substrate recognition by directly contacting precursor tRNA. *Proc. Natl Acad. Sci. USA*, **95**, 15212-15217.
- Platis, I. E., Ermacora, M. R. & Fox, R. O. (1993). Oxidative polypeptide cleavage mediated by EDTA-Fe covalently linked to cysteine residues. *Biochemistry*, **32**, 12761-12767.
- Rana, T. M. & Meares, C. F. (1991). Transfer of oxygen from an artificial protease to peptide carbon during proteolysis. *Proc. Natl Acad. Sci. USA*, **88**, 10578-10582.
- Sakano, H., Yamada, S., Ikemura, T., Shimura, Y. & Ozaki, H. (1974). Temperature-sensitive mutants of *Escherichia coli* for tRNA biosynthesis. *Nucl. Acids Res.* **1**, 355-371.
- Sanderson, M. R., Freemont, P. S., Rice, P. A., Goldman, A., Hatfull, G. F., Grindley, N. D. & Steitz, T. A. (1990). The crystal structure of the catalytic domain of the site-specific recombination enzyme gamma delta resolvase at 2.7 Å resolution. *Cell*, **63**, 1323-1329.
- Sandman, K., Grayling, R. A. & Reeve, J. N. (1995). Improved N-terminal processing of recombinant proteins synthesized in *Escherichia coli*. *Biotechnology*, **13**, 504-506.
- Stams, T., Niranjanakumari, S., Fierke, C. & Christianson, D. W. (1998). Ribonuclease P protein structure: evolutionary origins in the translational apparatus. *Science*, **280**, 752-756.
- Talbot, S. J. & Altman, S. (1994). Gel retardation analysis of the interaction between C5 protein and M1 RNA in the formation of the ribonuclease P holoenzyme from *Escherichia coli*. *Biochemistry*, **33**, 1399-1405.
- Tullius, T. D. (1987). Chemical 'snapshots' of DNA: using the hydroxyl radical to study the structure of DNA and DNA-protein complexes. *Trends Biochem. Sci.* **12**, 297-300.
- Yang, W. & Steitz, T. A. (1995). Crystal structure of the site-specific recombinase gamma delta resolvase complexed with a 34-bp cleavage site. *Cell*, **82**, 193-207.

Edited by K. Nagai

(Received 26 August 1999; received in revised form 30 November 1999; accepted 8 December 1999)